Journal of Materials Chemistry A

Accepted Manuscript

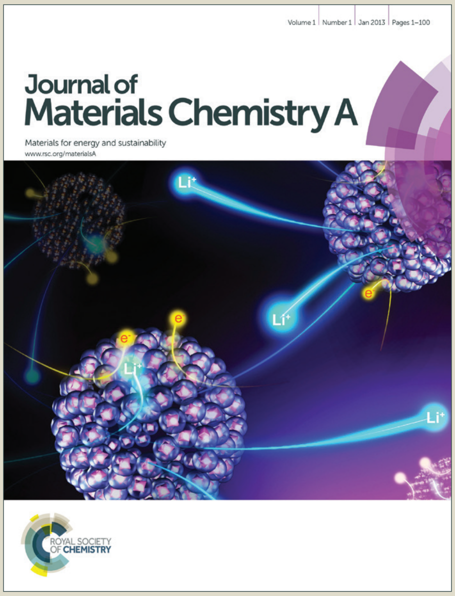

ROYAL SOCIETY OF CHEMISTRY

www.rsc.org/materialsA

Journal Name RSCPublishing

ARTICLE

Cite this: DOI: 10.1039/x0xx00000x

Received 00th January 2012,
Accepted 00th January 2012

DOI: 10.1039/x0xx00000x

www.rsc.org/

Improving the Permeance of Hybrid Polymer/ Metal Organic Framework (MOF) Membranes for Organic Solvent Nanofiltration (OSN) – Development of MOF Thin Films via Interfacial Synthesis

James Campbell[a,b], R.P. Davies[b], Chris Braddock[b], A.G. Livingston[a]*

In-situ growth (ISG) of metal organic frameworks (MOFs) within the pores of integrally skinned asymmetric polymer membrane supports has previously been shown to outperform mixed matrix membranes (MMMs) for organic solvent nanofiltration (OSN) applications. However these membranes have the disadvantage of low flux performances. In order to improve solvent permeance through hybrid MOF/Polymer membranes a fabrication methodology to produce MOF thin film composite membranes (MOF-TFCs) has been developed. Interfacial synthesis was utilised to produce a thin layer of HKUST-1 on polyimide P84 ultrafiltration supports. Two different fabrication methodologies were employed; methodology A resulted in the HKUST-1 layer growing above the polymer membrane surface and methodology B resulted in HKUST-1 growth embedded in the surface of the polymer support membrane. The MOF-TFCs produced via methodology A were shown to have similar solute retentions as ISG membranes; however the permeance values achieved were over 3 times higher than that of the ISG membranes.

1. Introduction

The increased interest in porous crystalline materials, known as metal organic frameworks (MOFs), over the last 15 years has been accompanied by a co-current rise in the development of separation processes utilising these materials. Within membrane science research there has been significant interest in using MOFs as molecular sieves, especially in gas separations, however, due to their crystalline nature, pure MOFs membranes are too brittle for real world applications. To combat this, hybrid polymer/MOF membranes have been developed utilising the flexibility and mechanical strength of polymer membranes while incorporating the separation potential of MOFs.

Mixed matrix membranes (MMMs) are the most common hybrid polymer/MOF membranes, used mostly for gas separation applications[1-6]. MMMs are made by dispersing pre-formed MOF particles in polymer membrane dope solutions[4] leading to the formation of membranes with discrete particles distributed in a continuous polymer phase[4]. MMMs containing MOFs have also been produced for organic solvent nanofiltration (OSN) applications; their porous nature utilised to improve the performance of thin film composite membranes[7, 8]. MOFs have also been integrated into the structure of integrally skinned asymmetric membranes to produce MMMs, also tested in organic solvent conditions[9]. While MMMs are easily fabricated, their separation performances will never be able to reach that of pure MOF membranes due to their structural properties. As MMMs contain discrete inorganic particles, there are no continuous permeation pathways of MOF throughout the membranes and therefore the permeation properties of the membranes are determined by both the polymer and MOF. MMMs can also suffer from imperfect interaction between the surfaces of the MOF particles and the polymer matrix. This can lead to the formation of non-selective voids, rigid polymer layers and polymer incursion into the MOF, which can reduce the effectiveness of the membranes[7, 10-12].

To combat the issues associated with MMMs a methodology known as in-situ growth (ISG) has been developed to produce hybrid polymer/MOF membranes[9, 13-15]. First developed for gas separation processes, in-situ growth has been shown to improve the performance of membrane above that of pure polymeric membranes and mixed matrix membranes[13-15]. ISG membranes have also been shown to outperform MMMs for organic solvent nanofiltration (OSN) applications[9]. However these membranes have the disadvantage of low flux performances. ISG membrane fabrication leads to the growth of thick MOF phases, which restricts solvent permeation. A simple solution to improve the permeances of hybrid polymer/MOF membranes would be to reduce the thickness of the MOF separation layer.

Thin film composite (TFC) membranes consist of a thin selective layer on top of a separate porous support layer made from a different material[16]. TFC membranes have higher fluxes as compared to integrally-skinned asymmetric membranes due to their ultrathin selective layers, and the highly porous support layers which offer little resistance to solvent flux. TFC membranes are commonly fabricated utilising interfacial synthesis, a process which was first described in the early 1980s by Cadotte *et al.*[17, 18]. TFC membranes are extensively used in desalination because of their high permeance values and solute retentions[19-24]. TFC membranes have also been fabricated for OSN applications[25-29]. The permeance performances of hybrid inorganic/polymer membranes containing MOFs have also been improved by fabricating thin MOF films via interfacial synthesis.

Most MOF film fabrication processes have focused either on direct growth via solvothermal synthesis onto a substrate surface, or layer by layer deposition[30-33]. These methodologies can lead to the formation of thick films (over 10 microns), with defects, and are difficult to scale-up. Forming MOF thin films via interfacial synthesis is likely to result in thinner films, with fewer defects. Ameloot *et al.* developed a methodology to fabricate hollow capsules of HKUST-1 using interfacial synthesis[34], the MOF films surrounding these capsules were under 1 micron thick and defect free. During interfacial synthesis the reagents primarily meet and react at the site of any remaining defects, meaning films are self-completing.

Forming thin MOF films via interfacial synthesis can be achieved using the same technology used to produce commercial polymer TFC membranes. Interfacial synthesis has been used to create membranes used for gas separation processes[35, 36]. Using a two-step process and solvothermal synthesis, films of ZIF-8 were grown on the surface of porous alumina disks[36]. ZIF-8 thin films were also grown on polymer hollow fibre membranes, demonstrating the ability to create polymer/MOF thin film hybrid membranes[35]. ZIF-8 thin films formed via interfacial synthesis have also been used for OSN separations, achieving high retentions for Rose Bengal in water, ethanol and iso-propyl alcohol[37].

This paper reports on the fabrication of thin films of MOF HKUST-1 on Polyimide P84 support membranes via interfacial synthesis. The HKUST-1 thin film hybrid membranes were compared to ISG membranes for OSN separations in order to ascertain whether producing thin film membranes could improve solvent permeances.

The thin film fabrication methodology used was based on work carried out by Ameloot *et al.*[34]. Two fabrication methodologies were devised in order to ascertain the influence of solvent positioning on film fabrication; methodology A and B. This work expands upon the work of Brown *et al.*[35] and Li *et al.*[37], who both created hybrid membranes using ZIF-8, by proving that HKUST-1 thin films can also be formed on the surface of polymer support membranes. While tested in OSN conditions, these membranes could potentially also be used in gas separations and catalytic processes.

2. Experimental Details

2.1. Materials

Polypropylene non-woven backing was supplied by Viledon, Germany. Polyimide polymer (Polyimide P84) powder was purchased from HP Polymer GmbH, Austria. Solvents used for membrane preparation and membrane testing, isopropyl alcohol (IPA), acetone, dimethylformamide (DMF), ethanol (99.7%) and polyethylene glycol (MW 400) (PEG-400) were obtained from VWR international. Octanol was purchased from Sigma Aldrich. Hexane-1,6-diamine for crosslinking was purchased from Sigma Aldrich. Copper nitrate trihydrate, copper acetate monohydrate and 1,3,5-benzenetricarboxylic acid used for HKUST-1 fabrication were purchased from VWR international. Polystyrene markers for solute rejection evaluation were purchased from Agilent Technologies, UK. All the chemicals were used as received without any further purification.

2.2. Membrane Preparation

2.2.1. Preparation of polymer ultrafiltration UF) membranes Polymer ultrafiltration (UF) membranes were produced via phase inversion. Dope solutions were formed by dissolving 24 wt% of polyimide P84, herein referred to as P84, in DMF. The P84 and the DMF were mixed in a sealed container, while the polymer dissolved, to ensure no moisture was absorbed into the dope solution. The dope solutions were cast on to polypropylene non-woven sheets using a casting knife set to a thickness of 250 μm in a controlled environment with a temperature of 20 °C and a humidity of 30–40%. The polymer membranes were then precipitated from solution via immersion in water. The membranes were then placed in IPA to remove water from the polymer matrix. For crosslinking, the membranes were submerged in 30 g L^{-1} solutions of hexane-1,6-diamine (HDA) in IPA for 20 hours. After crosslinking the membranes were washed with IPA to remove excess crosslinking agent. Before testing, the membranes were conditioned with a PEG400:IPA (60:40 v/v) solution for 12 hours.

2.2.2. Preparation of hybrid polymer/MOF membranes via In-situ growth (ISG) of HKUST-1 Hybrid polymer/MOF membrane fabricated via in-situ growth (ISG) were fabricated using polymer UF membranes as structural scaffolds. ISG membranes were prepared by immersing the polymer UF membranes into a fresh mixture of copper nitrate (0.86 M in Ethanol solution) and 1,3,5-benzenetricarboxylic acid (0.40 M in DMF solution) solution. The membranes were left stirring in solution for 24 hours, and were then extensively washed with DMF to remove any unreacted reagents. Before testing the membranes were conditioned with a PEG400:IPA (60:40 v/v) solution for 12 hours.

2.2.3. Preparation of hybrid polymer/MOF thin film membranes MOF thin film composite membranes (MOF-TFCs) were produced via interfacial synthesis of a HKUST-1 film on a P84 polymer ultrafiltration membrane. The thin film fabrication methodology was based on the work carried out by Ameloot *et al.*[34]. Two fabrication methodologies were devised in order to ascertain the influence solvent position on film fabrication.

Fabrication Methodology A

A piece of P84 UF membrane was soaked in a 70 g L^{-1} solution of copper acetate in water. The membrane was removed from the solution, and excess solution removed from the surface of the membrane. The membrane was then taped to the bottom of a petri dish and a 17 g L^{-1} solution of 1,3,5-benzene tricarboxylic acid in octanol poured on top of the membrane.

Fabrication Methodology B

A piece of P84 UF membrane was soaked in a 17 g L^{-1} solution of 1,3,5-benzenetricarboxylic acid in octanol. The membrane was removed from the solution, and excess solution removed from the surface of the membrane. The membrane was then taped to the bottom of a petri dish and a 70 g L^{-1} solution of copper acetate in water poured on top of the membrane.

Before testing, membranes were conditioned with a PEG400:IPA (60:40 v/v) solution for 12 hours.

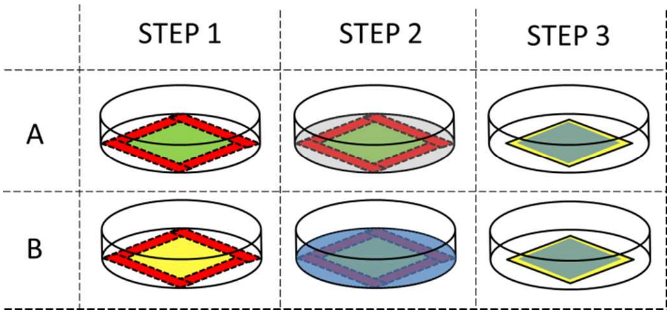

Figure 1: Schematic representation of fabrication method A, wherein the P84 support membrane is impregnated with copper acetate in water and of fabrication method B wherein the P84 support membrane is impregnated with benzene tricarboxylic acid in octanol.

Figure 1 shows how the MOF thin films were prepared on the surface of the polyimide membranes. The membranes are initially taped to the bottom of a petri dish by tape (shown in red). In Step 1 the membrane impregnated by copper acetate is green (method A), while the membrane impregnated by benzene tricarboxylic acid remains yellow (method B). In Step 2 the membranes are completely covered by BTC in octanol solution (method A) and copper acetate in aqueous solution (method B). In Step 3 the tape is removed and the uncovered membranes have changed colour to blue.

2.3. Membrane Characterisation

2.3.1. Scanning electron microscopy/Energy-dispersive X-ray spectroscopy The samples were coated with chromium under an argon atmosphere using an Emitech K575X peltier in order to make the samples conductive. The microscopic analyses were performed at 5 kV in a high resolution LEO1525 Karl Zeiss SEM. Energy-dispersive X-ray spectroscopy (EDX) was carried out using the same LEO1525 Karl Zeiss SEM at 20 kV. The EDX samples were also coated with chromium.

2.3.2. ATR-FTIR Fourier Transform-Infrared (FT-IR) spectra were recorded on a Perkin-Elmer Spectrometer 100, with samples mounted on a zinc-selenium/diamond plate. The spectra were collected in the attenuated total reflection (ATR) mode, directly from the membrane surface. The spectra were recorded at a resolution of 4 cm^{-1} as an average of 16 scans. The membranes were washed in acetone to remove any contamination and dried before analysis.

2.4. Copper Acetate Solubility and Diffusion Measurements

A saturated solution of copper acetate was produced by adding an excess mass of copper acetate (0.0118g) to 20 ml of octanol, the solution was left for 48 hours, to maximise dissolution. Visible copper acetate crystals could be seen at the bottom of the solution, ensuring that the solution was saturated. The concentration of the saturated solution was measure using a Shimazdu UV-1800 UV-Vis spectrophotometer. The diffusion of copper acetate from aqueous solutions to octanol was found by adding pure octanol to aqueous 70 g L^{-1} solutions of copper acetate. As the liquids are immiscible, and octanol has a lower density than water, the octanol floated on top of the aqueous solution. After periodic time intervals the concentration of copper acetate in the octanol solutions was measured using the same Shimazdu UV-1800 UV-Vis spectrophotometer.

2.5. OSN experimental procedure

All filtration experiments were carried out at 10 bar using a cross-flow filtration system. The effective area of each membrane was 14 cm^2, and at least 2 discs of each membrane were placed in an 8 cell cross-flow rig, which comprises 2 parallel sets of 4 membranes in series. The membranes were tested for 24 hours in order to ensure a steady permeance had been reached. The membrane permeance was calculated as given in Equation 1.

$$Permeance = \frac{J}{\Delta P} = \frac{V}{\Delta P A t} = [L.m^{-2}.h^{-1}.bar^{-1}] \qquad \textbf{(Eq. 1)}$$

The permeance of each membrane was obtained by measuring the solvent flux through the membrane (J) and dividing this by the applied pressure across the membrane (ΔP). The flux was calculated by measuring the volume of solution (V) that permeates through the membrane per unit area (A) per unit time (t). The model system for the solute rejection experiments comprised of a mixture of 1 g L^{-1} PS580 and PS1300 polystyrene markers as well as 0.1 g L^{-1} of methyl styrene dimer solution in acetone[37]. The rejection ($R_{j,i}$) of markers was found by measuring the concentration of each polystyrene oligomer in the permeate ($C_{p,i}$) and the feed ($C_{f,i}$), respectively and calculating the ratio of the molecules retained by the membrane. The equation to calculate membrane rejection can be found in Equation 2.

$$R_{j,i} = \left(1 - \frac{C_{p,i}}{C_{f,i}}\right) \cdot 100 = [\%] \qquad \textbf{(Eq. 2)}$$

Samples of polystyrene solution were taken from the feed and the permeate line of each of the membranes. The acetone was evaporated and the residue was re-dissolved in DMF. The HPLC analysis was based on the method previously reported by

See-Toh et al[37]. Analysis of the polystyrene markers was undertaken using an Agilent HPLC system equipped with UV/Vis detector set at a wavelength of 264 nm and a Phenomenex C18 (300A, 250x4.6 mm) reverse phase column.

3. Results

3.1 Fabrication Methodology A

The initial colour of the UF membrane impregnated with copper acetate was green. After exposure to the octanol/benzene tricarboxylic acid solution the membrane colour changed to blue. The colour change suggests that a layer of HKUST-1 MOF had grown on the surface of the membrane. However cracks appeared in the HKUST-1 film and the MOF layer delaminated from the membrane surface, revealing the polymer below. This is shown in **Figure 2**.

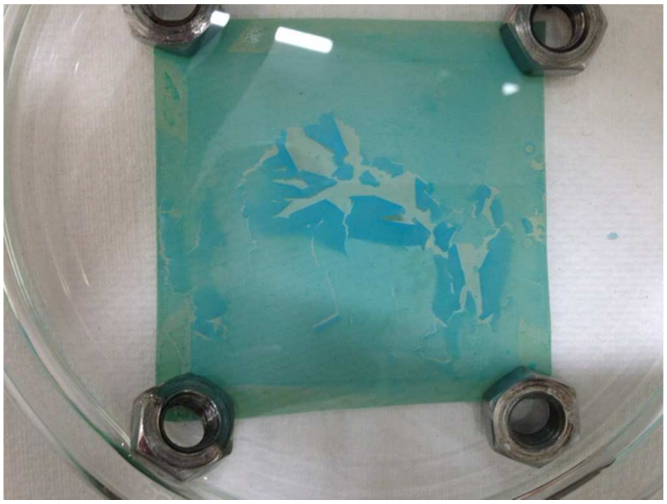

Figure 2: Methodology A; Cracking HKUST-1 layer caused by overgrowth of MOF layer on top of a P84 support membrane

The HKUST-1 MOF layer is brittle and does not chemically bond to the polymer support layer beneath. In order to produce membranes that can be used for OSN applications the HKUST-1 film must be firmly attached to the polymer support membrane.

Copper acetate was found to be slightly soluble in octanol, reaching saturation at 0.645 ± 0.08 g L^{-1}. It is theorized that the HKUST-1 crystallisation reaction occurs just above the aqueous/organic interface (See **Figure 3a**). Copper acetate molecules could diffuse across the interface from the water solution inside the membrane into the octanol solution and react with the 1,3,5-benzenetricarboxylic acid. The diffusion of copper acetate from concentrated aqueous solutions into octanol was measured over time (see **Figure 3b**). After just a short time the concentration of copper acetate in the octanol portion of the solutions had reached values comparable to saturated solutions.

Due to the diffusion of copper acetate into octanol over time it is possible that the HKUST-1 formation reaction occurs just above the membrane surface when methodology A is employed. If the reagent mixtures are alternated, and the 1,3,5-benzenetricarboxylic acid solution is impregnated in the membrane the copper acetate molecules will diffuse into the membrane and the film should grow within the polymer matrix.

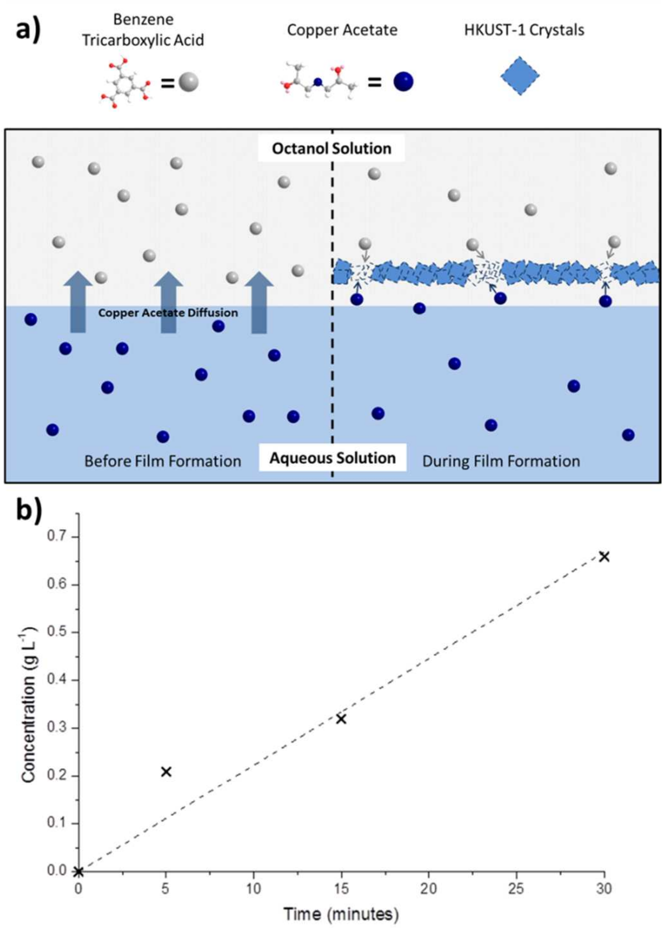

Figure 3: (a) Diagram demonstrating the diffusion of copper acetate molecules causing the MOF film to be formed on the octanol side of the solution. (b) Concentration with time of copper acetate in octanol solution. The copper acetate concentration increases over time due to diffusion from a 70 g L^{-1} aqueous solution of copper acetate. The black crosses represent the measured copper acetate concentrations at given times. The black dashed line shows the trend line of increasing copper acetate concentration.

3.2 Fabrication Methodology B

After 24 hours of exposure to the copper acetate solution the polyimide P84 membrane, impregnated with 1,3,5-benzenetricarboxylic acid in octanol, turned from yellow to blue. SEM images (see **Figure 4c & d**) show a dark band of HKUST-1 at the surface of the membrane. SEM-EDX confirms that the concentration of copper peaks sharply at the surface of the MOF-TFC (see **Figure 4g**), with another apparent peak at the bottom of the membrane. The copper peak at the base of the membrane can be explained by copper acetate solution leaking through gaps between the tape and membrane. This is in stark contrast to the SEM-EDX of the ISG membrane (see **Figure 4h**), for which there is a high concentration of copper throughout the middle of the membrane. The SEM-EDX results suggest that using immiscible solutions of water and octanol restricts the reaction of HKUST-1 to the surfaces of the membrane.

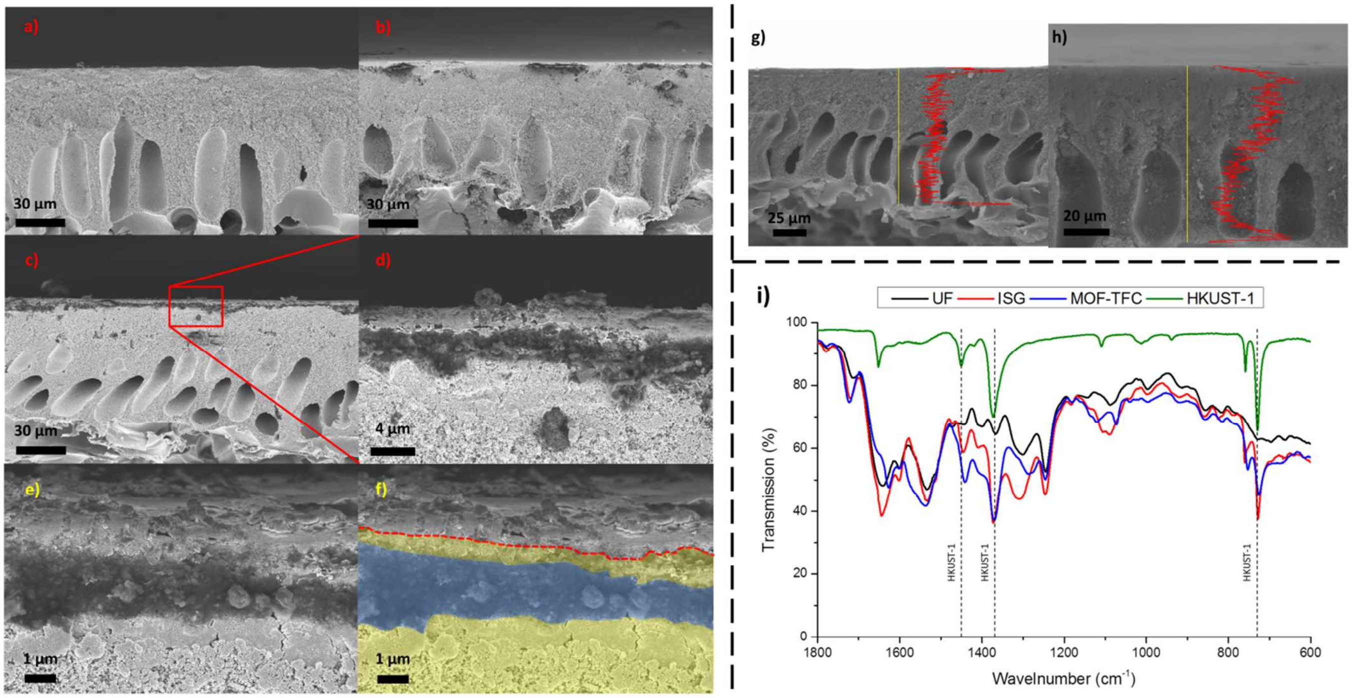

Figure 4: SEM cross-section images of (a) the UF membrane at magnification 1500x, (b) the ISG membrane at magnification 1500x and (c) the MOF-TFC membrane at magnification 1500x (d) and 10000x magnification; (e) SEM cross-section image of MOF-TFC membrane produced via methodology B, (f) is the same image highlighted to show the MOF layer (blue), the cross-sectional surface of the membrane (yellow) and the edge of the membrane where the membrane surface meeting the cross-section (red dotted line); SEM-EDX images of (g) the MOF-TFC membrane and (h) the ISG membrane, in which the red lines represent the concentration of copper throughout the cross-section of the membranes; (i) ATR-FTIR Spectra for UF, ISG and MOF-TFC membrane fabricated via methodology B, indicating that HKUST-1 has been successfully incorporated onto the surface of the MOF-TFC membrane.

Exploring the structure of MOF-TFC membranes further, the SEM image in **Figure 4e & f,** suggests that the MOF film grows just beneath the surface of the membrane. As previously discussed it is theorized that copper acetate molecules migrate across the liquid/liquid interface from the water solution into the octanol solution. As the octanol solution is inside the membrane, the MOF film grows just inside the membrane surface when fabrication methodology B is employed. This means that the HKUST-1 layer is firmly embedded in to the membrane structure. As the MOF film is physically embedded into the polymer layer the brittle nature of HKUST-1 is negated and therefore cracks and defects are less likely to occur post-film fabrication.

Figure 4i shows the ATR-FTIR spectra for the membranes as compared to the spectrum pure HKUST-1 powder. ATR-FTIR was used to confirm the presence of HKUST-1 in the MOF-TFC membranes. Due to the thinness of the MOF film in the MOF-TFCs, the mass of HKUST-1 within the membranes was too low to be adequately detected using X-ray powder diffraction (XRPD). ATR-FTIR can only penetrate the surface of the membranes up to 5 microns, therefore is can be used to analyse the chemistry of only the surface of the membrane. The characteristic peaks of HKUST-1 bonds are identified as occurring at 740, 1380 and 1450 cm^{-1}. While the UF membrane displays no evidence of peaks at these wavenumbers, both the ISG and MOF-TFC membranes have peaks which occur at these points.

Table 1 shows the thickness, mass and density of the pure polymer membrane (UF), uncontrolled *in-situ* growth membrane (ISG) and the thin film MOF membrane (MOF-TFC). The change in mass and density of the MOF-TFC membrane is significantly less than the changes measured for the ISG membrane, indicating that there is less MOF in the MOF-TFC membrane. Less HKUST-1 material has grown in the MOF-TFC, as the crystal growth is restricted to a thin band at the surface of the membrane. The MOF-TFC membranes fabricated via methodology B were found to be flexible as the MOF film is embedded in the polymer film, and thus the membranes were tested in OSN conditions.

Table 1: Thickness, mass and density of Membranes

Membrane	**Thickness (µm)**	**Mass (g m^{-2})**	**Density (g cm^{-3})**
UF	100	57	0.57
ISG	107	88	0.82
MOF-TFC	101	62	0.61

Figure 5 shows that synthesis of MOF films via interfacial synthesis does not adversely affect the selective nature of HKUST-1 as compared to *in-situ* growth, as the solute retentions of the MOF-TFC and ISG membrane are similar. **Table 2** shows that the MOF-TFC membrane has a permeance over three times as high as the ISG membrane. Producing a thin MOF film, rather than the undirected growth of the ISG membrane, reduces the resistance to flow in the membranes, resulting in higher permeance performances.

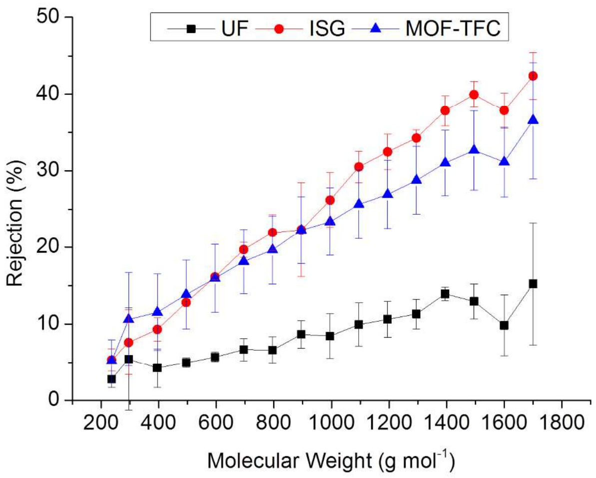

Figure 5: Rejection of polystyrene markers in acetone at 10 bar applied pressure. Mean data for each membrane plotted, error bars show one standard deviation

Table 2: Permeance data for the membranes tested at 10 bar

Membrane	Permeance ($L\ m^{-2}\ h^{-1}\ bar^{-1}$)
UF	131 ± 11
ISG	16.1 ± 0.9
MOF-TFC	54.0 ± 16.0

The performance of the MOF-TFC membrane indicates that this hybrid membrane fabrication methodology is an improvement on ISG for OSN applications, and by extension MMMs. While retention results are just as high for MOF-TFCs as they are for ISG membranes, the permeance performances are over three times higher.

4. Conclusions

This work shows that there is potential for using hybrid thin film MOF/polymer membranes for organic solvent nanofiltration (OSN) applications. Two methodologies were employed to produce MOF-TFC membranes, however only methodology B led to the fabrication of membranes suitable for testing in OSN conditions. Interfacial synthesis via methodology A led to the formation of brittle HKUST-1 layers on the outer surface of the membranes. SEM/EDX analysis showed that using methodology B led to HKUST-1 growth within the membrane surface.

MOF-TFC membranes were found to have higher solute retentions than polymeric ultrafiltration membranes, demonstrating that the MOF thin film had augmented the selective layer of the polymer membrane. MOF-TFCs were shown to have similar retentions to the existing ISG hybrid polymer/MOF membrane fabrication methodology, however solvent fluxes were over 3 times higher since the thin MOF selective layer is less restrictive to solvent flow.

Filtration experiments were carried out over a period of 24 hours maximum, and so the long term (over weeks and months) stability of ISG and MOF-TFC membranes are not currently known. Solvent co-ordination has been shown to affect the properties of HKUST-1, including porosity and crystallinity[38]. HKUST-1 has been shown to have low stability in water[39], but the stability of the MOF in organic solvents is unknown. Future tests should examine the long term stability of MOF-TFC and ISG membranes in OSN conditions.

The rejections achieved with the MOF-TFC membranes were not as high as desired i.e. 90 to 100% in the nanofiltration range (200 to 1000 g mol^{-1}). One simple way to improve the performances of these membranes would be to increase the solute retention of the polymer base membrane. Previous work by the authors investigating the formation of ISG membranes has shown that using dense ultrafiltration membranes as supports the performance of hybrid membranes could be improved[9]. The same approach could be applied to the formation of MOF-TFCs to improve the rejections achieved, although it would most likely result in a concomitant loss in permeance.

Further work should investigate the effect of altering the concentration of the reactive phases and the HKUST-1 film formation reaction time on membrane performances. If the extent of the reaction and subsequent growth of the HKUST-1 layer in MOF-TFCs is dependent on time and the interfacial solution concentrations, the performance of the membranes could be improved. Reducing the reaction time could reduce the thickness of the MOF films, increasing membrane permeances. Reducing the concentration of reagents could also improve the kinetics of HKUST-1 formation, possibly allowing films to form via methodology A without cracks forming, leading to improved solute rejections.

ATR-FTIR was used to confirm the presence of HKUST-1 in the MOF-TFCs, however the purity of the films cannot be determined using this methodology. XRPD could be used to determine the purity of the MOF films, ascertaining whether the film formation methodology may need to be altered to improve the structure of the HKUST-1 formed.

Acknowledgements

The authors would like to acknowledge financial support provided by the EPSRC, UK - DTA awards EP/P504953/1; EP/P505550/1; Platform Grant award EP/J014974/1 and the financial support from the Pharmacat Consortium.

Notes and references

[a] Department of Chemical Engineering, Imperial College, London SW7 2AZ, UK.

[b] Department of Chemistry, Imperial College, London SW7 2AZ, UK

∗ Corresponding author: Tel.: +44-20-7594-5582. *E-mail address:* a.livingston@imperial.ac.uk

1. A. Car, C. Stropnik and K.-V. Peinemann, Desalination, 2006, 200, 424-426.
2. H. B. T. Jeazet, C. Staudt and C. Janiak, Dalton Transactions, 2012, 41, 14003-14027.
3. J. Hu, H. Cai, H. Ren, Y. Wei, Z. Xu, H. Liu and Y. Hu, Industrial Chemical Engineering Research, 2010, 12605–12612.
4. G. Dong, H. Lia and V. Chen, Journal of Materials Chemistry A, 2013, 1, 4610–4630.
5. E. V. Perez, K. J. B. Jr., J. P. Ferraris and I. H. Musselman, Journal of Membrane Science, 2009, 328, 165–173.

6. Z. Zhao, X. Ma, A. Kasik, Z. Li and Y. S. Lin, Industrial & Engineering Chemistry Research, 2013, 53, 1102−1108.
7. S. Basu, M. Maes, A. Cano-Odena, L. Alaerts, D. E. D. Vos and I. F. J. Vankelecom, Journal of Membrane Science, 2009, 344, 190–198.
8. S. Sorribas, P. Gorgojo, C. Téllez, J. Coronas and A. G. Livingston, Journal of the American Chemical Society, 2013, 135, 15201–15208.
9. J. Campbell, G. Szekely, R. P. Davies, D. C. Braddock and A. G. Livingston, Journal of Materials Chemistry A, 2014, 2, 9260-9271.
10. L. Cao, K. Tao, A. Huang, C. Kong and L. Chen, Chemical Communication, 2013, 8513-8515.
11. L. Ge, W. Zhou, V. Rudolph and Z. Zhu, Journal of MAterials Chemistry A, 2013, 1, 6350–6358.
12. T.-S. Chung, L. Y. Jiang and S. K. Yi Lia, Progess in Polymer Science, 2007, 32, 483–507.
13. D. Nagaraju, D. G. Bhagat, R. Banerjee and U. K. Kharul, Journal of Materials Chemistry A, 2013, 1.
14. L. Ge, W. Zhou, A. Du and Z. Zhu, The Journal of Physical Chemistry C, 2012, 116, 13264−13270.
15. F. Cacho-Bailo, B. Seoane, C. Téllez and J. Coronas, Journal of Membrane Science, 2014, 464, 119–126.
16. R. J. Petersen, Journal of Membrane Science, 1993, 83, 81-150.
17. J. E. Cadotte, R. J. Petersen, R. E. Larson and E. E. Erickson, Desalination, 1980, 32, 25-31.
18. R. E. Larson, J. E. Cadotte and R. J. Petersen, Desalination, 1981, 38, 473–483.
19. K. P. Lee, T. C. Arnot and D. Mattia, Journal of Membrane Science, 2011, 370, 1-22.
20. W. J. Lau, A. F. Ismail, N. Misdan and M. A. Kassim, Desalination, 2012, 287, 190-199.
21. M. Liu, S. Yu, J. Tao and C. Gao, Journal of Membrane Science, 2008, 325, 947–956.
22. B. J. A. Tarboush, D. Rana, T. Matsuura, H. A. Arafat and R. M. Narbaitz, Journal of Membrane Science, 2008, 325, 166–175.
23. N. Misdan, W. J. Lau and A. F. Ismail, Desalination, 2012, 287, 228–237.
24. C. E. M. P.L. Riley, A.L. Lloyd, M.W. Seroy, M. Tagami, Desalination, 1977, 23, 331–355.
25. I.-C. Kim, J. Jegal and K.-H. Lee, Journal of Polymer Science Part B: Polymer Physics, 2002, 40, 2151–2163.
26. A. P. Korikov, P. B. Kosaraju and K. K. Sirkar, Journal of Membrane Science, 2006, 279, 588-600.
27. P.B.Kosaraju and K.K.Sirkar, Journal of Membrane Science, 2008, 321, 155–161.
28. P.B.Kosaraju and K.K.Sirkar, Journal of Membrane Science, 2007, 288, 41–50.
29. M. F. J. Solomon, Y. Bhole and A. G. Livingston, Journal of Membrane Science, 2012, 423-424, 371–382.
30. D. Zacher, O. Shekhah, C. Woll and R. A. Fischer, Chemical Society Reviews, 2009, 38, 1418–1429.
31. M. C. So, S. Jin, H.-J. Son, G. P. Wiederrecht, O. K. Farha and J. T. Hupp, Journal of American Chemical Society, 2013, 135, 15698−15701.
32. O. Shekhah, L. Fu, R. Sougrat, Y. Belmabkhout, A. J. Cairns, E. P. Giannelis and M. Eddaoudi, Chemical Communications, 2012, 48, 11434-11436.
33. O. Shekhah, J. Liu, R. A. Fischer and C. Woll, Chemical Society Reviews, 2011, 40, 1081–1106.
34. R. Ameloot, F. Vermoortele, W. Vanhove, M. B. J. Roeffaers, B. F. Sels and D. E. D. Vos, Nature Chemistry, 2011, 3, 382-387.
35. A. J. Brown, N. A. Brunelli, K. Eum, F. Rashidi, J. R. Johnson, W. J. Koros, C. W. Jones and S. Nair, Science, 2014, 345, 72-75.
36. H. T. Kwon and H.-K. Jeong, Journal of American Chemical Society, 2013, 135, 10763−10768.
37. Y. Li, L. H. Wee, A. Volodin, J. A. Martens and I. F. J. Vankelecom, Chemical Communication, 2014, 51, 918--920.
38. Y. Yang, P. Shukla, S. Wang, V. Rudolph, X.-M. Chen and Z. Zhu, RSC Advances, 2013, 3, 17065–17072.
39. P. Küsgens, M. Rose, I. Senkovska, H. Fröde, A. Henschel, S. Siegle and S. Kaskel, Microporous and Mesoporous Materials, 2009, 120, 325-330.